Supporting Information

Triallyl isocyanurate enabled SPAN-based organosulfur featuring high sulfur& selenium loading for advanced Li/Na−S batteries

Qiang Wu,[a] Mingsheng Qin,[ab] Yuanke Wu,[ab] Haolin Zhu,[a] Shijie Cheng,[a] Jia Xie*[a]

[a]State Key Laboratory of Advanced Electromagnetic Technology, School of Electrical and Electronic Engineering, Huazhong University of Science and Technology, Wuhan, Hubei, 430074, P. R. China

[b]State Key Laboratory of Materials Processing and Die & Mould Technology, School of Materials Science and Engineering, Huazhong University of Science and Technology, Wuhan, Hubei, 430074, P. R. China

* Corresponding authors: xiejia@hust.edu.cn (Jia Xie)

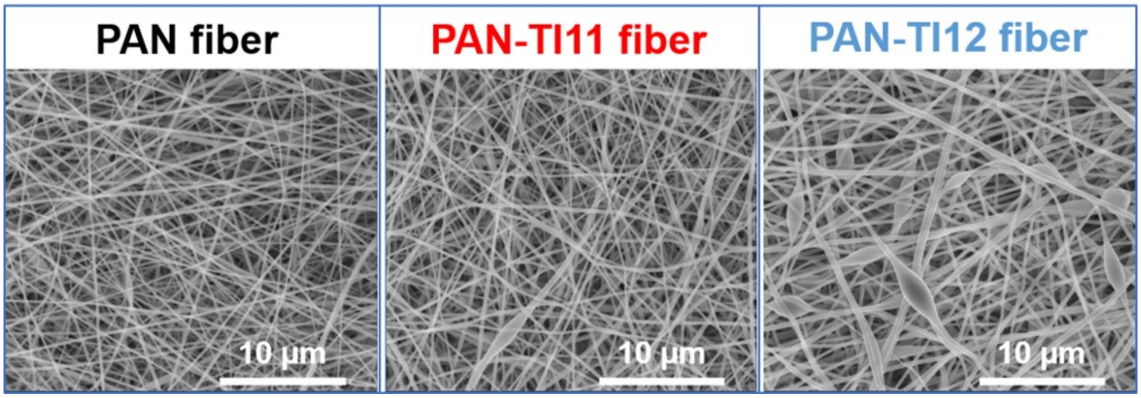

Fig. S1. SEM images of PAN fiber, PAN-TI11 fiber and PAN-TI12 fiber, respectively.

Table S1. Mass fraction of elements in 0F, 1F and 2F composites by elemental analysis.

Materials	C (%)	N (%)	H (%)	S (%)	Se (%)	S&Se (%)
0F	38.9	14.4	1.4	40.1	5.2	45.3
1F	34.2	1.1	10.5	47.9	6.3	54.2
2F	31.2	1.1	9.9	51.1	6.7	57.8

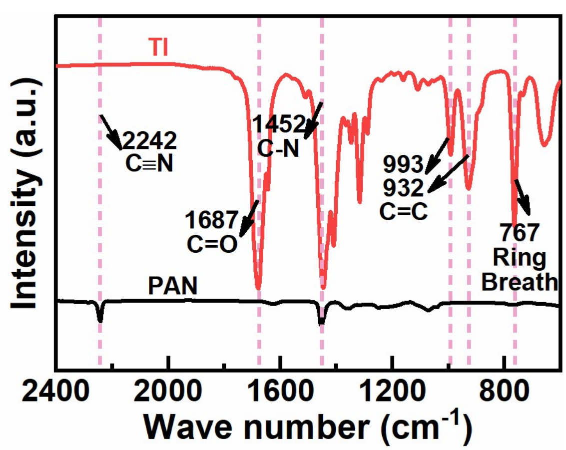

Fig. S2. FT-IR spectrum of TI and PAN.

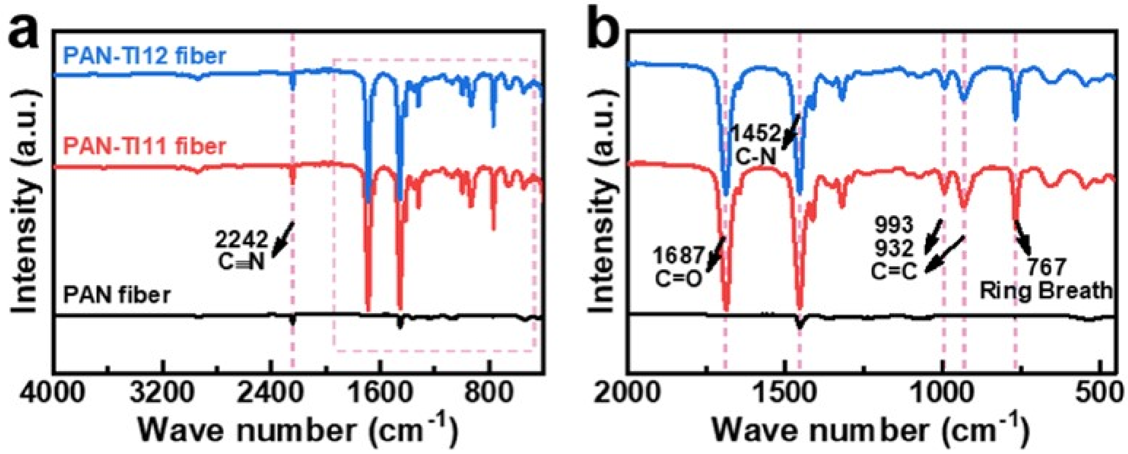

Fig. S3. (a) FT-IR spectrum of PAN fiber, PAN-TI11 fiber and PAN-TI12; (b) The partial enlarged FT-IR spectrum.

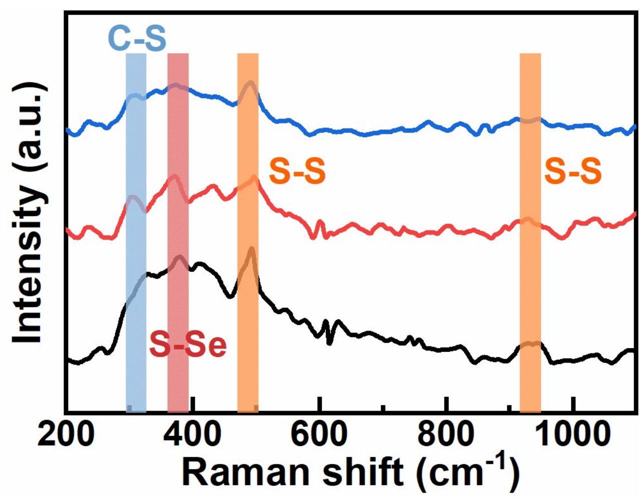

Fig. S4. Local enlarged Raman spectrums of $Se_{0.05}S_{0.95}$PAN fiber, $Se_{0.05}S_{0.95}$PAN-TI11 and 12 fibers.

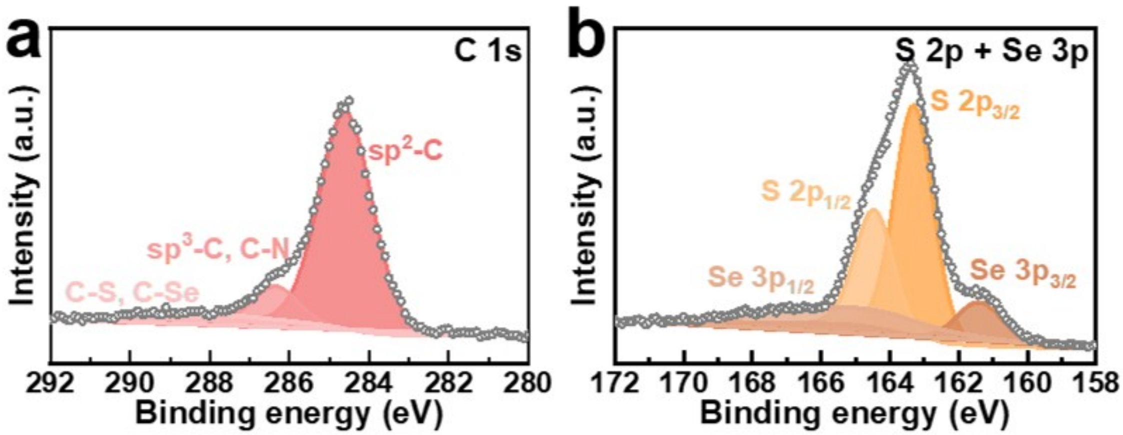

Fig. S5. (a) C 1s and (b) S 2p + Se 3p XPS spectra of $Se_{0.05}S_{0.95}$PAN-TI12 fiber.

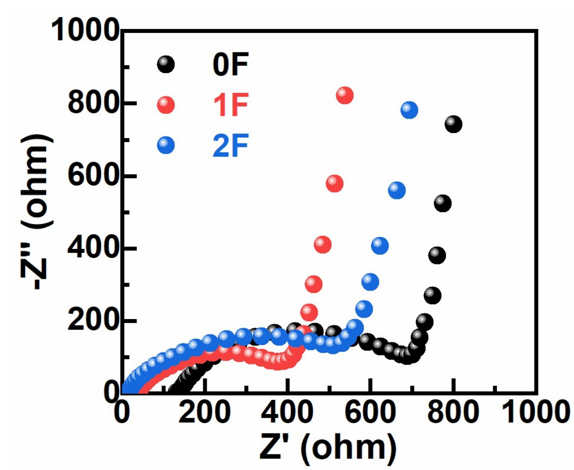

Fig. S6. The electrochemical impedance spectroscopy (EIS) of 0F, 1F and 2F.

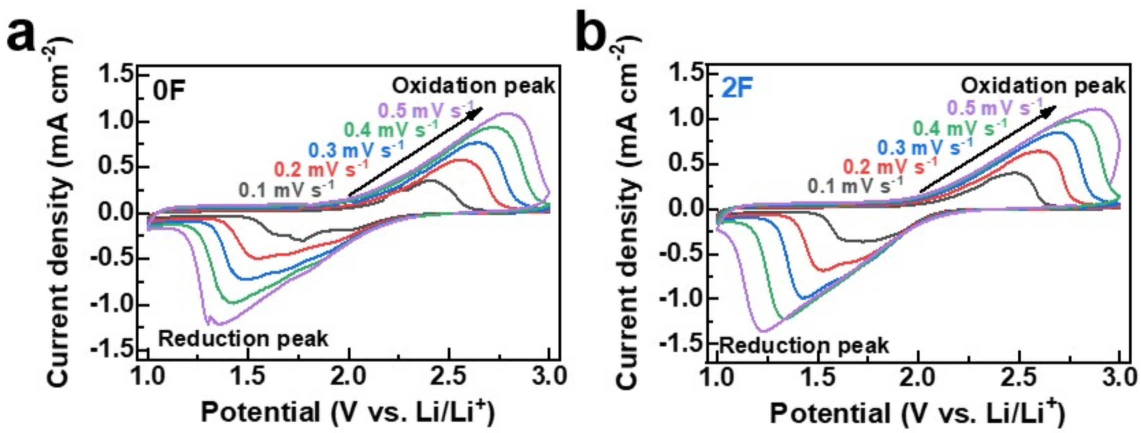

Fig. S7. CV curves of (a) 0F and (b) 2F from 0.1 to 0.5 mV s^{-1}.

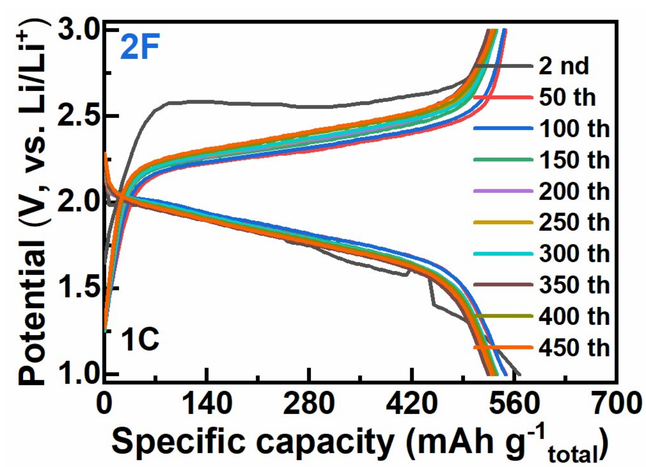

Fig. S8. The discharge-charge curves of 2F at various cycles.

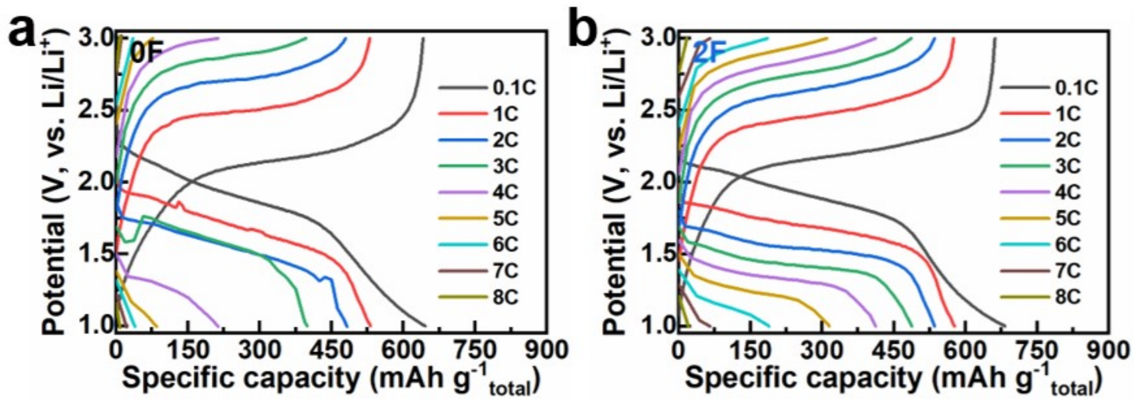

Fig. S9. The discharge-charge curves of (a) 0F and (b) 2F at various rates.

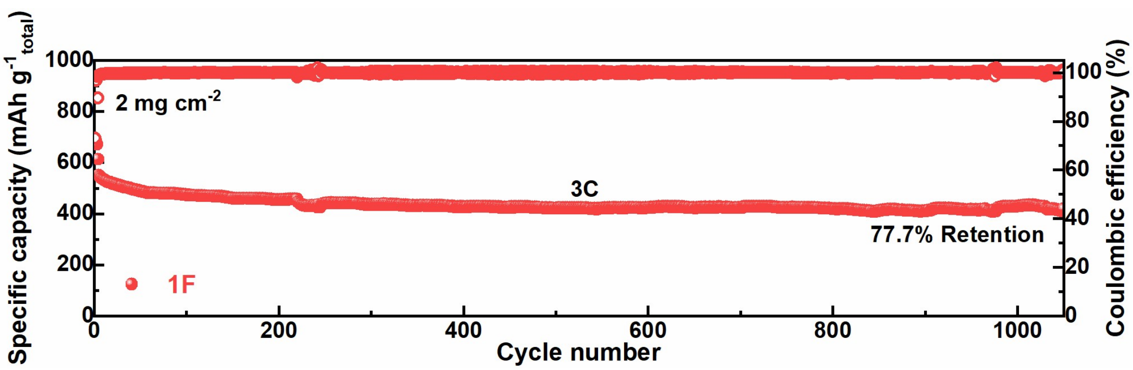

Fig. S10. Long cycling performance of 1F at 3C.

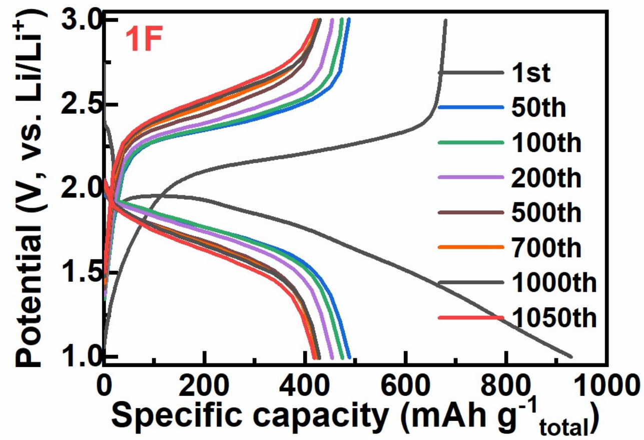

Fig. S11. The discharge-charge curves of 1F at different cycles.

Table S2. Cycle performance and high-rate capability of the 1F electrode compare with previously reported SPAN-based electrodes.

Cathode Materials	Reversible composite capacity (mAh g^{-1})	Capacity retention (%)	Rate capability (mAh g^{-1})	S&Se content (%)	Ref.
SVF	361.0(1C)	94.5(150cycle)	113.4(4C)	37.8%	1
	254.8(2C)	89.0(300cycle)			
I-S@pPAN	538(2C)	85.0%(1000cycle)	226.5(8C)	42.5%	2
CoS_2@-SPAN-CNT	380.2(1C)	98.8%(400cycle)	96.3(5C)	43.2%	3
SPAN	481.2(0.5C)	83.3%(350cycle)	\	40.1%	4
SPAN	450(0.5C)	99.3%(800cycle)	366.7(3C)	37.4%	5
$Se_{0.06}$SPAN	581.8(0.13C)	91.6%(500cycle)	427.5(6.5C)	47.3%	6
	572(0.26C)	72.8%(800cycle)			
FD/C-$Se_{0.05}S_{0.95}$PAN	602(1C)	96.3%(400cycle)	490.0(2.5C)	48.5%	7
pPAN/SeS_2	548.7(3.6C)	72.7%(2000cycle)	447.7(4.4C)	63.0%	8
SPAN-CNT-12	483.8(0.5C)	100%(800cycle)	362.9(1C)	41.0%	9
SPAN-CNT20	564.2(0.5C)	93.2%(250cycle)	403.0(5C)	40.3%	10
	554.1(1C)	79.8%(500cycle)			
H-SPAN	514.7(0.1C)	100%(300cycle)	205.6(1C)	41.2%	11
S@PAN/S_7Se	575.3(1.2C)	76.6%(500cycle)	453.6(3.6C)	68%	12
1F	627.1(1C)	97.4%(450cycle)	405.1(8C)	54.2%	This work
	526.7(2C)	89.4%(1000cycle)			

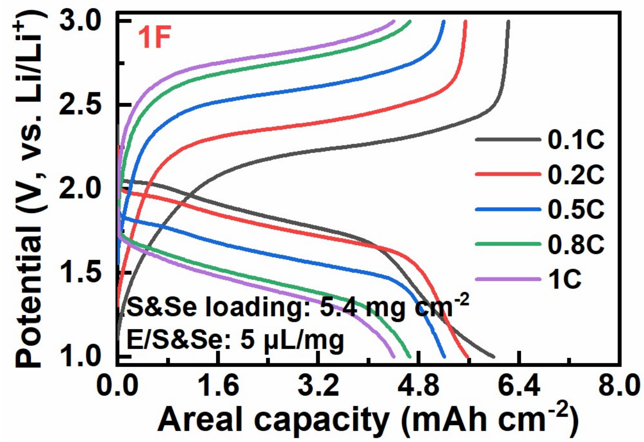

Fig. S12. The discharge-charge curves of 1F at different rates under practical conditions.

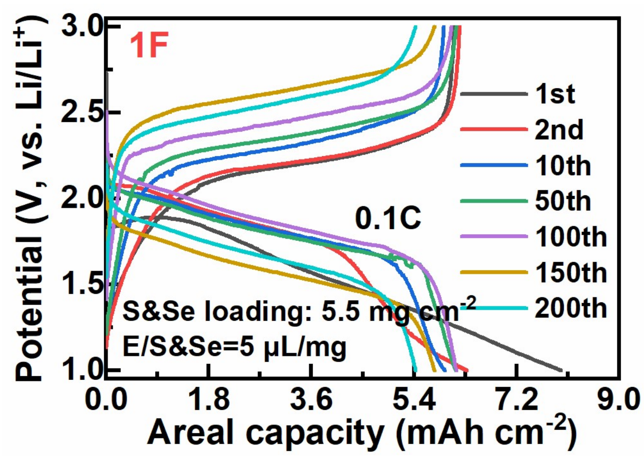

Fig. S13. The discharge-charge curves of 1F at different cycles under practical conditions.

Table S3. Comparison of the electrochemical performance of 1F with previously reported cathodes under harsh conditions.

Cathode Materials	S&Se loading (mg cm^{-2})	E/S (μL mg^{-1})	Areal capacity (mAh cm^{-2})	Capacity Retention (%)	Ref.
S@PAN/S_7Se	5.0	10	5	40 cycle (88%)	12
pPAN/SeS_2	5.0	50	4.5	50 cycle (90%)	8
$Se_{0.05}S_{0.95}$PAN	4.9	10	4.5	150 cycle (82%)	13
S/CTB/CNT-P10	6	4	4.6	100 cycle (75%)	14
G-g-sPS@S	6	15	6	50 cycle (69%)	15
AL-Lys-D cathode	5.75	20	4.2	150 cycle (69%)	16
1F	6.5	5	7	70 cycle (93%)	This work
	5.5	5	6	200 cycle (84%)	

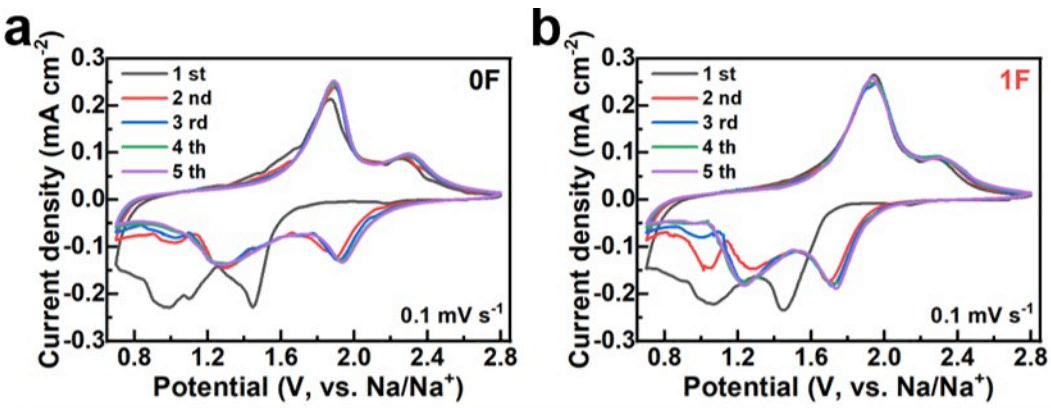

Fig. S14. The CV curves of (a) Na-0F battery and (b) Na-1F battery at 0.1 mV s^{-1}.

References

1 Y. Liu, A. K. Haridas, Y. Lee, K.-K. Cho and J.-H. Ahn, *Appl. Surf. Sci.* 2019, **472**, 135−142.

2 S. Ma, Z. Zhang, Y. Wang, Z. Yu, C. Cui, M. He, H. Huo, G. Yin and P. Zuo, *Chem. Eng. J.* 2021, **418**, 129410.

3 A. Abdul Razzaq, X. Yuan, Y. Chen, J. Hu, Q. Mu, Y. Ma, X. Zhao, L. Miao, J.-H. Ahn, Y. Peng and Z. Deng, *J. Mater. Chem. A* 2020, **8**, 1298−1306.

4 Z. Shen, W. Zhang, S. Mao, S. Li, X. Wang and Y. Lu, *ACS Energy Lett.* 2021, **6**, 2673−2681.

5 Y. He, P. Zou, S.-M. Bak, C. Wang, R. Zhang, L. Yao, Y. Du, E. Hu, R. Lin and H. L. Xin, *ACS Energy Lett.* 2022, **7**, 2866−2875.

6 X. Chen, L. Peng, L. Wang, J. Yang, Z. Hao, J. Xiang, K. Yuan, Y. Huang, B. Shan, L. Yuan and J. Xie, *Nat. Commun.* 2019, **10**, 1021.

7 Z. Han, S. Li, R. Xiong, Z. Jiang, M. Sun, W. Hu, L. Peng, R. He, H. Zhou, C. Yu, S. Cheng and J. Xie, *Adv. Funct. Mater.* 2022, **32**, 2108669.

8 Z. Li, J. Zhang, Y. Lu and X. W. Lou, *Sci. Adv.* 2018, **4**, eaat1687.

9 X. Wang, Y. Qian, L. Wang, H. Yang, H. Li, Y. Zhao and T. Liu, *Adv. Funct. Mater.* 2019, **29**, 1902929.

10 A. Abdul Razzaq, Y. Yao, R. Shah, P. Qi, L. Miao, M. Chen, X. Zhao, Y. Peng and Z. Deng, *Energy Stor. Mater* 2019, **16**, 194−202.

11 X. Huang, J. Liu, Z. Huang, X. Ke, L. Liu, N. Wang, J. Liu, Z. Guo, Y. Yang and Z. Shi, *Electrochim. Acta* 2020, **333**, 135493.

12 B. He, Z. Rao, Z. Cheng, D. Liu, D. He, J. Chen, Z. Miao, L. Yuan, Z. Li and Y. Huang, *Adv. Energy Mater.* 2021, **11**, 2003690.

13 Z. Jiang, Z. Zeng, X. Liang, L. Yang, W. Hu, C. Zhang, Z. Han, J. Feng and J. Xie, *Adv. Funct. Mater.* 2021, **31**, 2005991.

14 H. Chen, X. Zhang, S. Li and Y. Zheng, *ACS Energy Lett.* 2023, **8**, 619.

15 J. Wu, J. Huang, Y. Cui, D. Miao, X. Ke, Y. Lu and D. Wu, *Adv. Mater.* 2023, **35**, 2211471.

16 Z. Chen, M. Lu, Y. Qian, Y. Yang, J. Liu, Z. Lin, D. Yang, J. Lu and X. Qiu, *Adv. Energy Mater.* 2023, **13**, 2300092.